Supplementary Information

Cd/In-Codoped TiO_2 Nanochips for High-Efficiency Photocatalytic Dye Degradation

Dongliang Liu,[a] Peng Huang,[a] Yong Liu,[a] Zhou Wu,[a] Dongsheng Li,[b] Jun Guo,[c] and Tao Wu[a,*]

[a] *College of Chemistry, Chemical Engineering and Materials Science, Soochow University, Suzhou, Jiangsu 215123, China.*

[b] *College of Materials and Chemical Engineering, Hubei Provincial Collaborative Innovation Center for New Energy Microgrid, Key Laboratory of Inorganic Nonmetallic Crystalline and Energy Conversion Materials, China Three Gorges University, Yichang, Hubei 443002, China*

[c] *Testing & Analysis Center, Soochow University, Suzhou, Jiangsu 215123, China.*

* Corresponding author

Email: wutao@suda.edu.cn

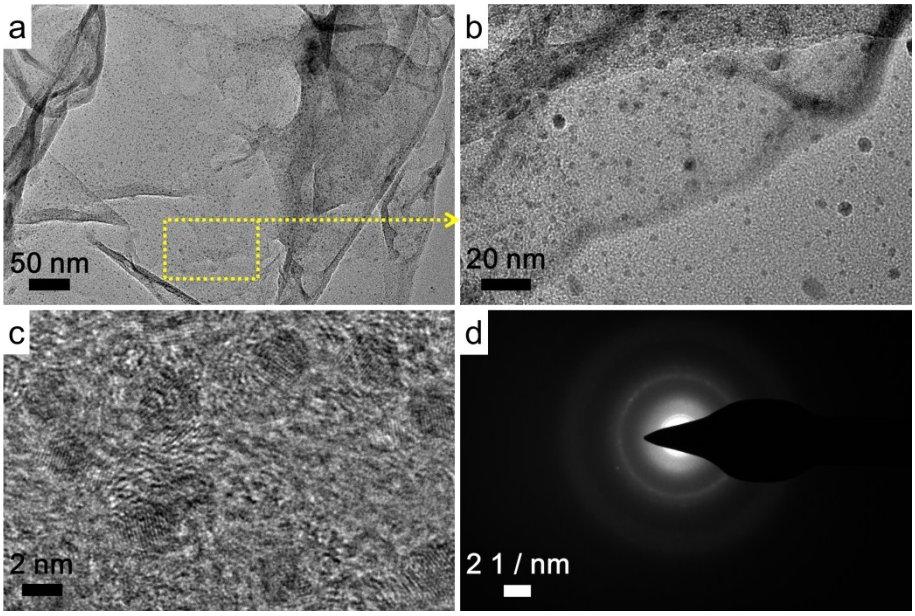

Fig. S1 TEM (a, b), HRTEM (c) images and SAED patterns (d) of Cd/In/S-TiO_2 gels.

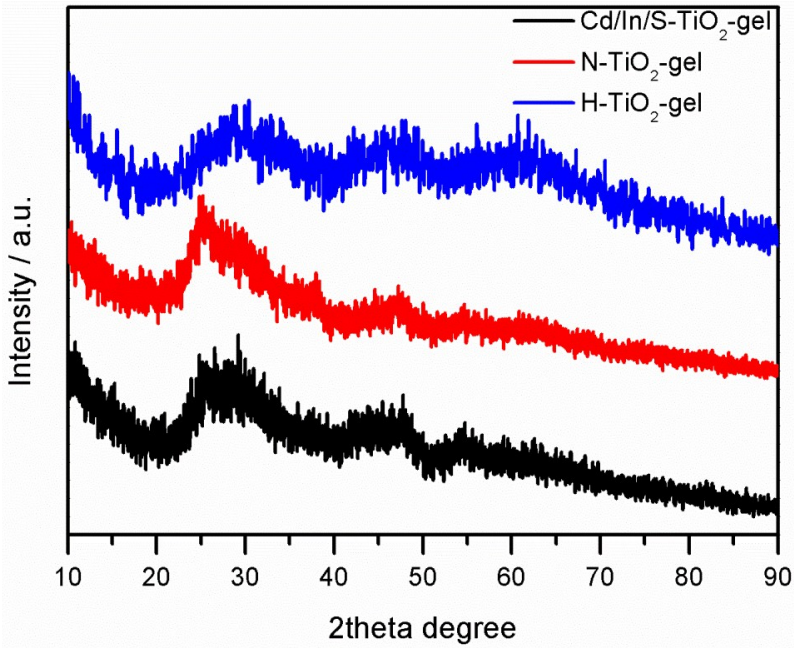

Fig. S2 XRD patterns of TiO_2 gels.

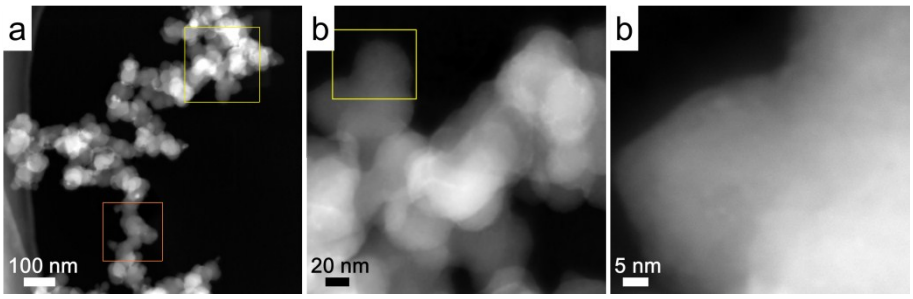

Fig. S3 STEM (a, b) and HRSTEM (c) images of Cd/In-TiO_2-700 nanochips.

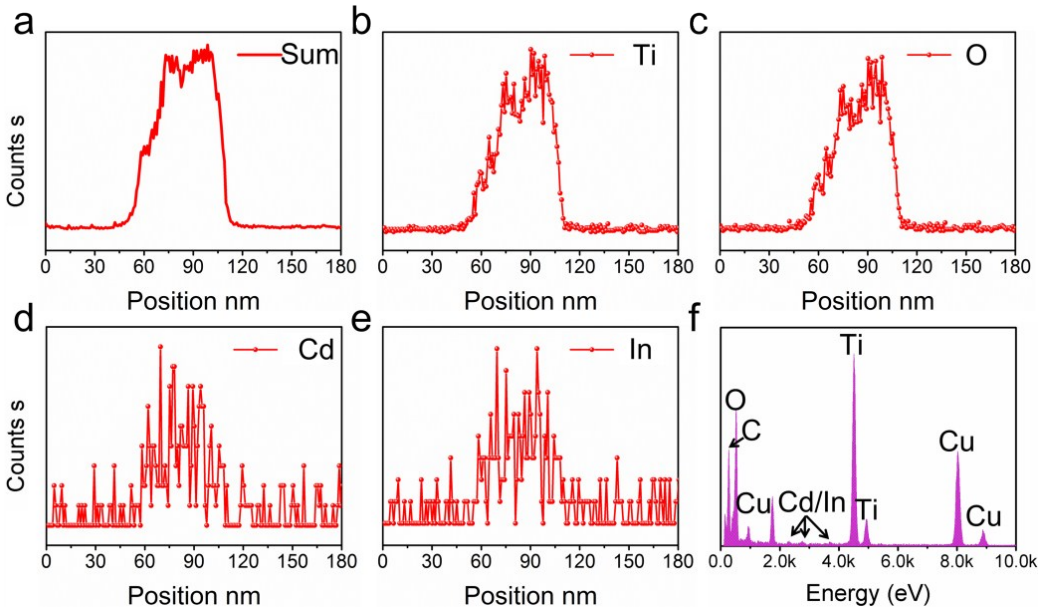

Fig. S4 STEM-line scans (a-e), and its corresponding EDS of Cd/In-TiO_2-700 nanochips.

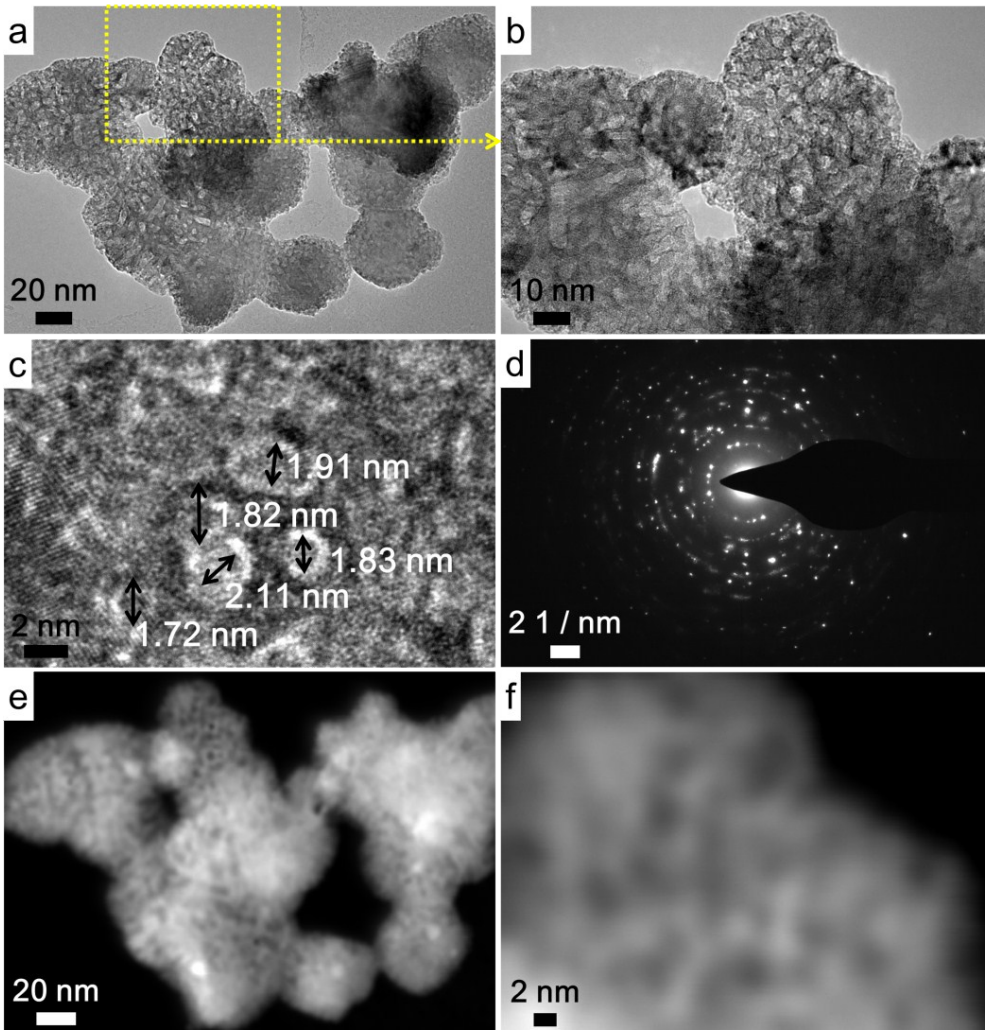

Fig. S5 TEM (a, b), HR-TEM (c), SAED (d), STEM (e) and HR-STEM (f) images of Cd/In-TiO_2-800 sample.

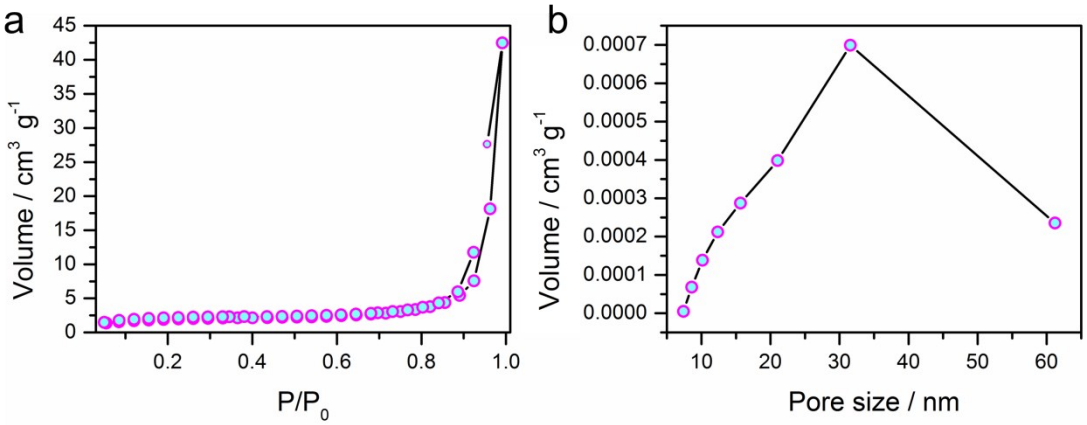

Fig. S6 N_2 adsorption-desorption isotherm (a) and the pore size distribution (b) of commercial TiO_2.

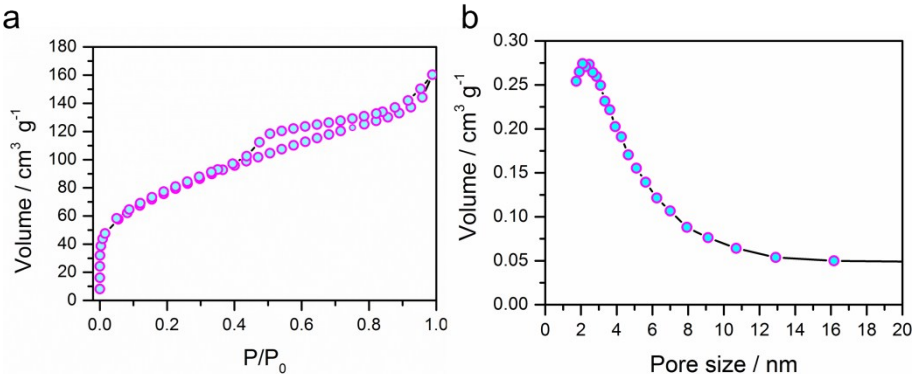

Fig. S7 N_2 adsorption-desorption isotherm (a) and the pore size distribution (b) of P25.

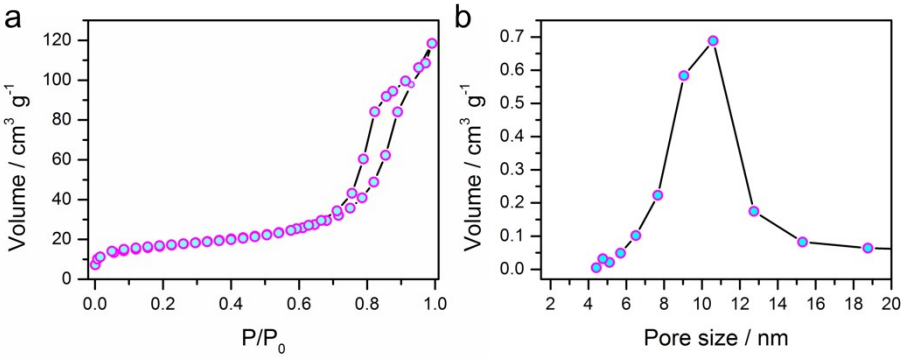

Fig. S8 N_2 adsorption-desorption isotherm (a) and the pore size distribution (b) of Cd/In/S-TiO_2 gel.

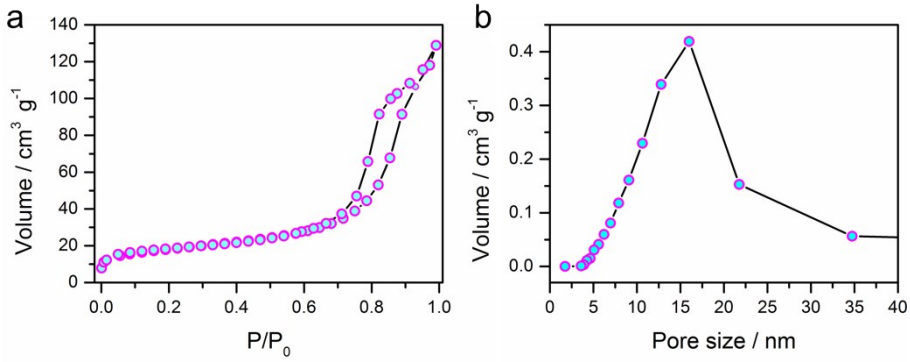

Fig. S9 N_2 adsorption-desorption isotherm (a) and the pore size distribution (b) of Cd/In-TiO_2-400.

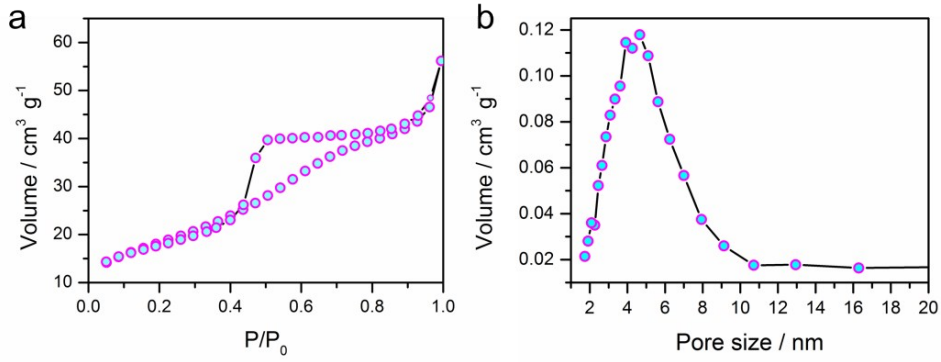

Fig. S10 N_2 adsorption-desorption isotherm (a) and the pore size distribution (b) of Cd/In-TiO_2-500.

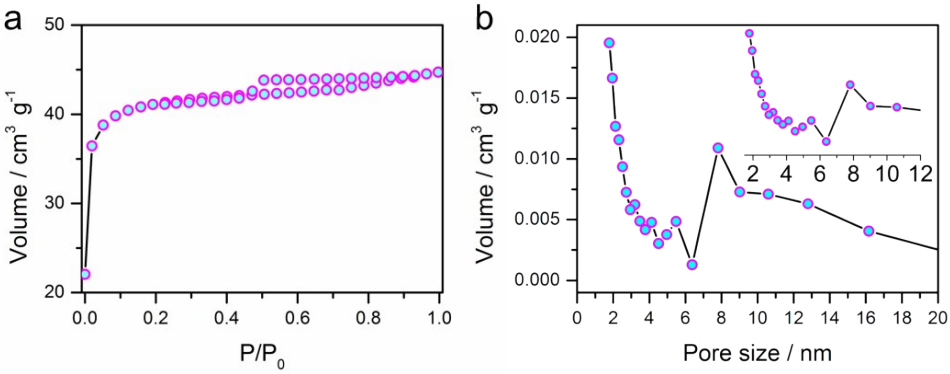

Fig. S11 N_2 adsorption-desorption isotherm (a) and the pore size distribution (b) of Cd/In-TiO_2-600.

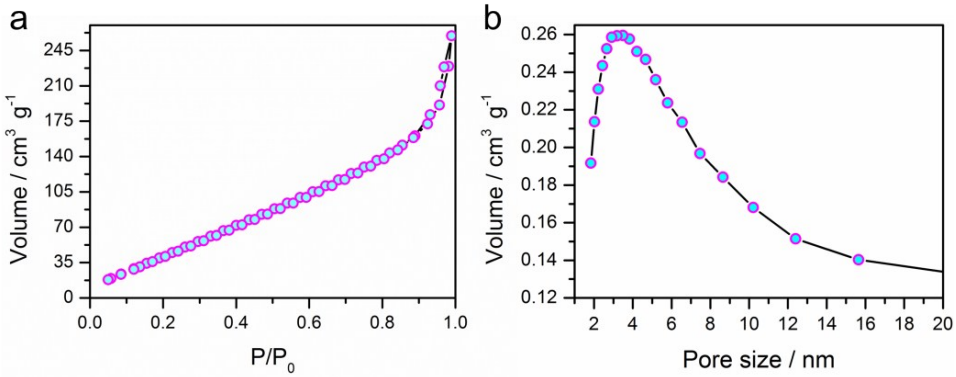

Fig. S12 N_2 adsorption-desorption isotherm (a) and the pore size distribution (b) of Cd/In-TiO_2-800.

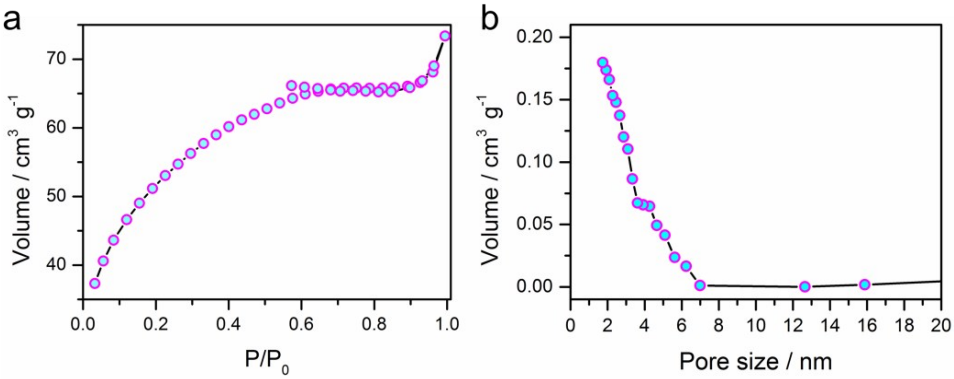

Fig. S13 N_2 adsorption-desorption isotherm (a) and the pore size distribution (b) of H-TiO_2-700.

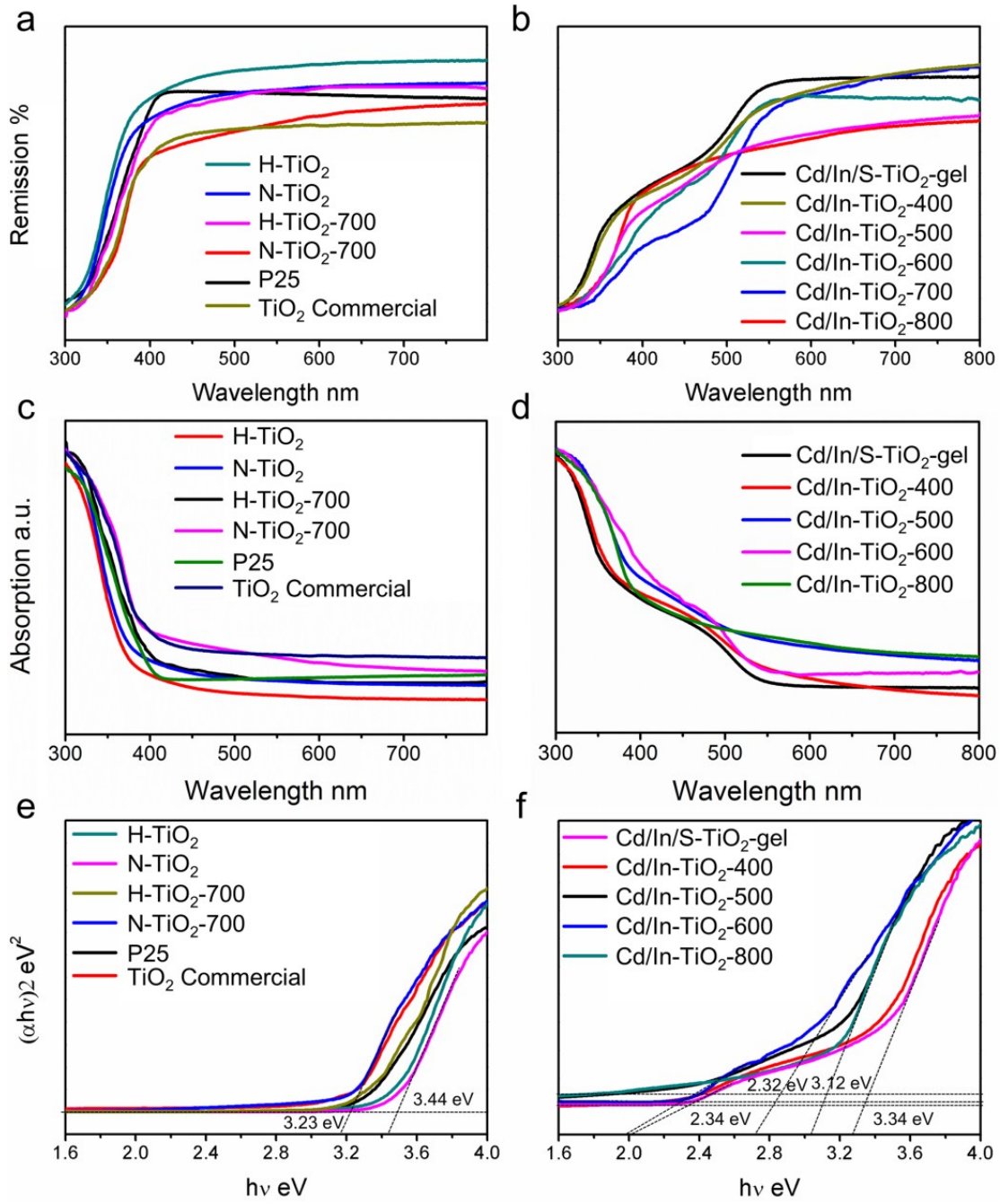

Fig. S14 UV-vis diffuse reflectance spectroscopy (a), UV-vis absorption (b) and plots of $(\alpha h\nu)^2$ versus photon energy for calculation of bandgap energy (c) of all TiO_2 samples.

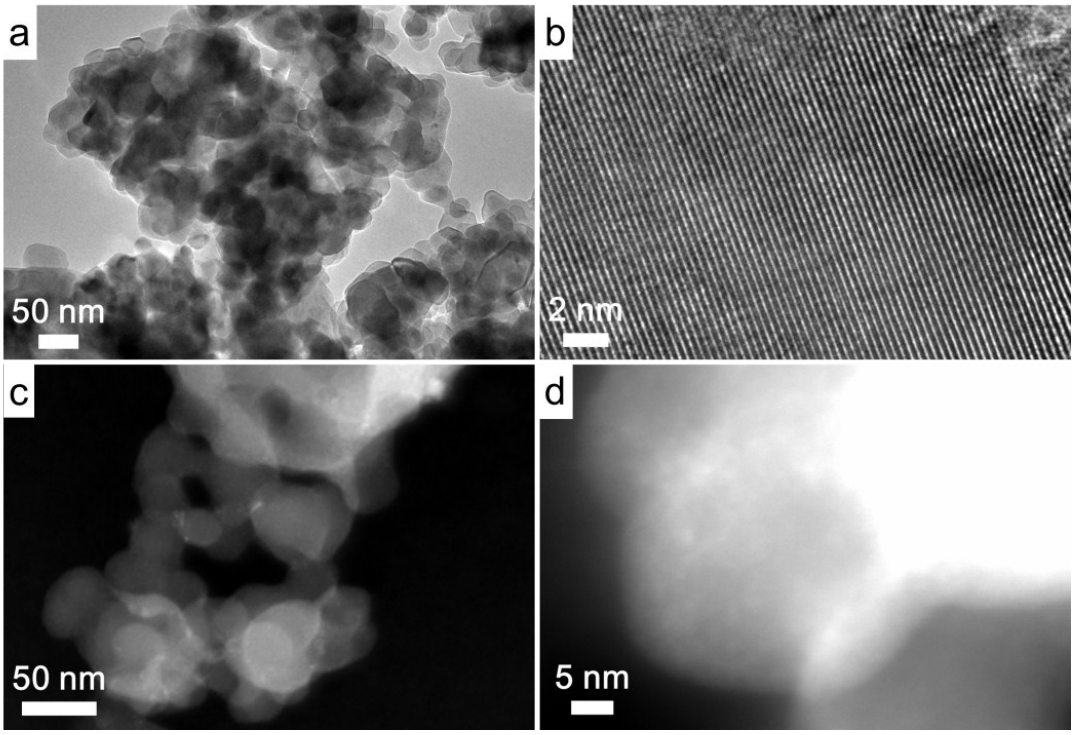

Fig. S15 TEM (a), HR-TEM (b), STEM (c) and HR-STEM (d) images of N-TiO_2-700 samples.

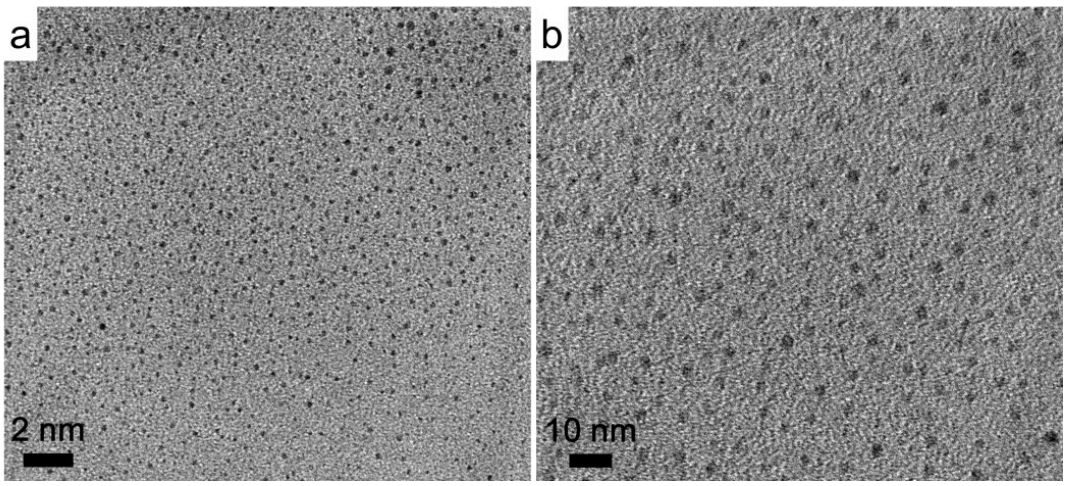

Fig. S16 TEM images of Cd-In-S nanocluster-based nanoparticles loaded on carbon film.

Table S1. ICP results of various TiO_2-based samples.

	Cd	In	Ti
Cd/In/S-TiO_2 gel	1.6	5.7	92.7
Cd/In-TiO_2-400	1.4	5.4	93.2
Cd/In-TiO_2-500	1.3	5.2	93.5
Cd/In-TiO_2-600	0.8	4.9	94.3
Cd/In-TiO_2-700	0.4	4.0	95.6
Cd/In-TiO_2-800	0	0	100

Table S2. BET surface areas of various TiO_2-based samples.

Samples	**Commercial TiO_2**	**P25**	**Cd/In/S-TiO_2 gel**	**Cd/In-TiO_2-400**	**Cd/In-TiO_2-500**
BET (m^2 g^{-1})	6.58	272	56.88	61.88	64.36
Samples	**Cd/In-TiO_2-600**	**Cd/In-TiO_2-700**	**Cd/In-TiO_2-800**	**H-TiO_2-700**	
BET (m^2 g^{-1})	176.77	215.54	216.37	131.49	

Table S3. Normalized Ka by BET surface area of various TiO_2-based samples.

Samples	**Cd/In/S-TiO_2 gel**	**Cd/In-TiO_2-400**	**Cd/In-TiO_2-500**
Ka/BET (m^{-2} g)	1.21 e^{-4}	1.26 e^{-4}	1.54 e^{-4}
Samples	**Cd/In-TiO_2-600**	**Cd/In-TiO_2-700**	**Cd/In-TiO_2-800**
Ka/BET (m^{-2} g)	0.7 e^{-4}	1.19 e^{-4}	0.97 e^{-5}